# Spontaneous and Stimulated Raman Scattering in Long Low Loss Fibers

JOHN AUYEUNG, STUDENT MEMBER, IEEE, AND AMNON YARIV, FELLOW, IEEE

*Abstract*—**This paper considers the problem of forward Raman scattering process in a single transverse mode fiber. Both pump wave depletion and spontaneous scattering are considered in the analysis. Analytic solutions of the governing differential equations are obtained. We examine the conditions under which a nondepleted pump approximation is valid. Expressions are derived for the maximum fiber loss and the minimum fiber length which allow significant pump to Stokes wave conversion. It is shown that for a given fiber length there is an optimal pumping power, or at a given pump power there is an optimal fiber length that yields maximum first-order Stokes power output. Good agreement with published experimental results in the threshold power prediction is obtained.**

## INTRODUCTION

RECENTLY, considerable research efforts have been directed towards the study of nonlinear optical effects in optical fibers. A low loss optical fiber is capable of guiding electromagnetic wave propagation over long distances, and at the same time, confining it to a small cross-sectional area, thus providing a long interacting region with large electric field intensity. This situation is especially favorable for nonlinear interactions. It was determined that threshold powers of a few watts are sufficient to cause nonlinear phenomena such as stimulated Raman and stimulated Brillouin scatterings [1]-[8]. Light sources operating at new wavelengths made possible by using the stimulated Raman or stimulated Brillouin scattering in fibers have been demonstrated. Owing to the large Raman scattering linewidth in glass, glass fiber tunable sources with a large tuning range in frequency have also been achieved [5]-[10]. Of particular importance is the recent demonstration of a tunable fiber Raman laser operating around 1.1 $\mu$m [8]-[10]. A silica fiber several hundred meters long, pumped by a Nd:YAG laser at 1.064 $\mu$m, was made to lase at 1.1 $\mu$m with a tuning range of 367 $cm^{-1}$ [8]. Such sources are potentially useful for studying fiber optic communication systems since both the absorption and the dispersion of silica fibers are near their minima in this wavelength region. Another reason for studying nonlinear effects in fibers is to understand their limitation in handling optical power [11]. Through nonlinear interaction, large optical powers will cause generation of unwanted frequencies, physical damage to the fiber, and especially signal distortions by phase modulation or crosstalk between different frequency components of the signal.

Manuscript received December 20, 1977. This work was supported by the Air Force Office of Scientific Research.

The authors are with the Department of Electrical Engineering, California Institute of Technology, Pasadena, CA 91125.

In this paper, we present a model for describing the stimulated Raman scattering process, in the forward direction, through a single transverse mode fiber. Pump wave depletion that is due to the nonlinear interaction, plus spontaneous scattering are both incorporated in our model. A previous analysis by Smith [11] which neglects pump depletion by the stimulated process but allows for linear absorption of the pump is found to be valid in the case of high loss fibers, which were the only ones available when Smith considered this problem. The neglect of pump depletion is not valid in treating today's low loss fibers (<4 dB/km); and the present analysis constitutes an extension to this practically important case.

## ANALYSIS

Consider the total pump power to be concentrated in only one pump mode and to be injected into the end of a single transverse mode fiber at $z = 0$. As this pump wave propagates along the fiber, it is depleted by linear absorption in the fiber as well as by down conversion to Stokes photons. The differential equation governing the pump wave photon number $n_p$ is

$$\frac{dn_p}{dz} + \alpha_p n_p = -\gamma_0 n_p (n_{s1} + 1 + n_{s2} + 1 + \cdots + n_{sq} + 1). \tag{1}$$

Subscripts $p$ and $s$ refer to the pump and Stokes photons. $\alpha_p$ is the absorption constant of the fiber at the pump wave frequency. $\gamma_0$ is the nonlinear gain constant associated with the Raman process. $n_{sj}$ is the photon number of the $j$th longitudinal Stokes modes. $q$ is the number of Stokes modes participating in the interaction. The integer 1 that goes with each Stokes mode accounts for the spontaneous scattering into that mode [12]. Each $n_{sj}$ obeys the equation

$$\frac{dn_{sj}}{dz} + \alpha_s n_{sj} = \gamma_0 n_p (n_{sj} + 1). \tag{2}$$

The total Stokes photon number is

$$n_s = \sum_{j=1}^{q} n_{sj} \tag{3}$$

and it satisfies the equation

$$\frac{dn_s}{dz} + \alpha_s n_s = \gamma_0 n_p (n_s + q). \tag{4}$$

$\alpha_s$ is the absorption constant of the fiber at the Stokes frequency. The initial conditions are

0018-9197/78/0500-0347$00.75 © 1978 IEEE

$$n_p(z=0) = n_{p0},$$

$$n_{sj}(z=0) = n_{sj0},$$

$$n_s(z=0) = \sum_{j=1}^{q} n_{sj0} = n_{s0}, \tag{5a}$$

and we define

$$n_0 = n_{p0} + n_{s0} \tag{5b}$$

to be the total input photon number.

In (1)-(5) we made the approximation that the gain constant $\gamma$ is the same for all the $q$ modes partaking in the interaction. The exact procedure would be to allow each Stokes mode $j$ to have a gain $\gamma_j = \gamma(\nu_j)$ which is proportional to the Raman line shape. The nondepleted pump analysis of Smith [11] shows that the correct result is obtained if we take $\gamma_j$ to be a constant over an effective Stokes input bandwidth $B_{\text{eff}}$ and take it as zero elsewhere. This is due to the combined frequency dependence of $\gamma(\nu_j)$ and the exponential nature of the amplification process which, together, discriminate strongly against Stokes modes removed from line center. In the presence of a finite Stokes wave input of bandwith $\Delta\nu_s$, the effective bandwidth, following Smith's analysis, is

$$B_{\text{eff}} = \frac{\Delta\nu_R}{2}\left[\frac{\pi}{\frac{\gamma_0 n_{p0}}{\alpha_p}\left[1 - \exp(-\alpha_p z)\right] + (\Delta\nu_R/\Delta\nu_s)^2}\right]^{1/2}. \tag{6}$$

$\Delta\nu_R$ is the Raman linewidth. In the absence of a Stokes wave input, any significant Stokes wave buildup at the fiber output end is due to single-pass superradiant emission. In this case,

$$B_{\text{eff}} = \frac{\Delta\nu_R}{2}\left[\frac{\pi}{\frac{\gamma_0 n_{p0}}{\alpha_p}\left[1 - \exp(-\alpha_p z)\right]}\right]^{1/2} \tag{7}$$

for large $z$. The effective number of Stokes modes $q$ is taken as the number of longitudinal fiber modes falling within $B_{\text{eff}}$ and is

$$q = n_{\text{eff}} \frac{L}{c} B_{\text{eff}}, \tag{8}$$

where $n_{\text{eff}}$ is the effective mode index of refraction (in practice essentially the fiber core index) and $L$ is the length of the fiber.

We have compared the results of the analysis based on the effective bandwidth concept to a numerical analysis using a frequency dependent gain. The results, described further on in the paper, justify the use of $B_{\text{eff}}$.

In most cases, Stokes shifts in fibers are confined to a region less than several hundred wave numbers [13] and hence $\alpha_p$ is nearly equal to $\alpha_s$. This is especially true in the 1 $\mu$m wavelength region where $\alpha$ is near its minimum and $d\alpha/d\lambda$ is small. We shall assume that this is indeed the case and let $\alpha_p = \alpha_s = \alpha$. Adding (1) and (4), we get

$$\frac{d}{dz}(n_p + n_s) + \alpha(n_p + n_s) = 0. \tag{9}$$

Hence, the total photon number varies as

$$n_p + n_s = n_0 \exp(-\alpha z). \tag{10}$$

This is merely a photon conservation statement indicating that the nonlinear interaction conserves photons; and a decrease in the total photon number is due solely to absorption in the fiber medium. Substituting (10) into (1) and (4), we have

$$\frac{dn_p}{dz} + n_p\left[\alpha + q\gamma_0 + \gamma_0 n_0 \exp(-\alpha z)\right] = \gamma_0 n_p^2 \tag{11}$$

and

$$\frac{dn_s}{dz} + n_s\left[\alpha + q\gamma_0 - \gamma_0 n_0 \exp(-\alpha z)\right] = -\gamma_0 n_s^2 + q\gamma_0 n_0 \exp(-\alpha z). \tag{12}$$

Equations (11), (12), and (2) with the initial conditions (5) can be solved exactly. The solutions (whose derivations are given in the Appendix) are

$$n_p(z) = \frac{n_0 \exp(-\alpha z)}{1 + \xi + \eta}, \tag{13}$$

$$n_s(z) = n_0 \exp(-\alpha z)\frac{\xi + \eta}{1 + \xi + \eta}, \tag{14}$$

$$n_{sj}(z) = \frac{n_0 \exp(-\alpha z)}{1 + \xi + \eta}\left(\frac{n_{sj0}}{n_{s0}}\xi + \frac{1}{q}\eta\right), \tag{15}$$

where

$$\xi = \frac{n_{s0}}{n_{p0}} \exp\left\{q\gamma_0 z + \frac{\gamma_0 n_0}{\alpha}\left[1 - \exp(-\alpha z)\right]\right\}, \tag{16}$$

and

$$\eta = q\gamma_0 \exp\left[q\gamma_0 z - \frac{\gamma_0 n_0}{\alpha}\exp(-\alpha z)\right] \cdot \sum_{l=0}^{\infty} \frac{\left(\frac{\gamma_0 n_0}{\alpha}\right)^l \left\{1 - \exp\left[-(l\alpha + q\gamma_0)z\right]\right\}}{(l\alpha + q\gamma_0)l!}. \tag{17}$$

$\xi(z)$ describes the conversion from pump to Stokes photons due to a finite Stokes photon input $n_{s0}$. $\eta(z)$, on the other hand, describes amplified spontaneous scattering.

For typical pumping powers of a few watts, $n_{p0} \gg q$ and $n_{p0} \gg n_{s0}$ so that $n_0 \approx n_{p0}$. The series in (17) can very well be approximated for large $z$ by $(1/\gamma_0 n_{p0}) \exp(\gamma_0 n_0/\alpha)$, and

$$\eta = \frac{q}{n_{p0}} \exp\left\{q\gamma_0 z + \frac{\gamma_0 n_0}{\alpha}\left[1 - \exp(-\alpha z)\right]\right\}. \tag{18}$$

We note that in this case, $\eta$ is identical to $\xi$ as given by (16) provided the input Stokes photon number $n_{s0}$ is taken to be $q$, that is, the spontaneous emission output can be viewed as due to an input of one Stokes photon per mode. It is apparent that the amplified spontaneous scattering can be modeled alternatively by ignoring the spontaneous effect altogether in the differential equations, provided an equivalent input of 1 photon per mode is assumed.

## Discussion

In order to relate our model to the experimental results, (13)-(18) are rewritten in terms of power. $P_p$ and $P_s$ are used to denote the power in the pump and Stokes waves, respectively. The change in the following notations in self-explanatory. Equations (13)-(18) become

$$P_p(z) = \frac{P_0 \exp(-\alpha z)}{1 + \xi + \eta}, \tag{19}$$

$$P_s(z) = \frac{\nu_s}{\nu_p} P_0 \exp(-\alpha z) \frac{\xi + \eta}{1 + \xi + \eta}, \tag{20}$$

$$P_{sj}(z) = \frac{\nu_s}{\nu_p} \frac{P_0 \exp(-\alpha z)}{1 + \xi + \eta} \left( \frac{P_{sj0}}{P_{s0}} \xi + \frac{1}{q} \eta \right), \tag{21}$$

$$\xi = \frac{\nu_p}{\nu_s} \frac{P_{s0}}{P_{p0}} \exp\left\{ \frac{g_s P_0}{\alpha A} [1 - \exp(-\alpha z)] \right\}; \tag{22}$$

and

$$\eta = \frac{\nu_p}{\nu_s} \frac{q h \nu_s v_g}{P_0 L} \exp\left\{ \frac{g_s P_0}{\alpha A} [1 - \exp(-\alpha z)] \right\}. \tag{23}$$

In (22) and (23), we have omitted a factor $\exp(q\gamma_0 z)$ which is close to 1 even for very large $z$. $P_0$ is defined to be $P_{p0} + (\nu_p/\nu_s)P_{s0}$. $\nu_p$ and $\nu_s$ are the pump and Stokes wave frequencies, respectively. $v_g$ is the group velocity in the fiber medium. $A$ is the effective cross-sectional area of the fiber. $g_s$ is the Raman power gain coefficient normally measured in experiments. $h$ is Planck's constant.

Let us consider some of the consequences of (19)-(23). When $\xi + \eta \ll 1$,

$$P_p(z) \simeq P_0 \exp(-\alpha z). \tag{24}$$

In this limit, the conversion to Stokes photons is negligible and $P_p(z)$ according to (24) is attenuated only by the fiber loss $\alpha$. When $\xi + \eta \gg 1$,

$$P_s(z) \simeq \frac{\nu_s}{\nu_p} P_0 \exp(-\alpha z). \tag{25}$$

The conversion is completed and all the pump power has been transferred to Stokes power. When $(\nu_s/\nu_p)(\xi + \eta) = 1$, $P_p$ equals $P_s$. We define this condition as the threshold condition. The input pump power which causes $(\nu_s/\nu_p)(\xi + \eta) = 1$ at $z = L$ is referred to as the threshold power. When $P_0 \simeq P_{p0} \gg P_{s0}$,

$$\frac{\nu_s}{\nu_p}(\xi + \eta) = \frac{1}{P_0} \left( P_{s0} + \frac{q h \nu_s v_g}{L} \right) \cdot \exp\left\{ \frac{g_s P_0}{\alpha A} [1 - \exp(-\alpha z)] \right\}. \tag{26}$$

Fig. 1 shows $(\nu_s/\nu_p)[\xi(z) + \eta(z)]$ for different values of $\alpha$. The parameters used in plotting the curves are $P_0 = 1$ W, $P_{s0} = 0$, $\lambda_p = 1.06$ $\mu$m, $\lambda_s = 1.12$ $\mu$m, $\Delta\nu_R = 400$ cm$^{-1}$, $g_s = 5 \times 10^{-10}$ cm/W, and $A = 10^{-7}$ cm$^2$. For $\alpha z \gg 1$,

$$\frac{\nu_s}{\nu_p}(\xi + \eta) = \frac{P'}{P_0} \alpha^{1/2} \exp\left( \frac{g_s P_0}{\alpha A} \right), \tag{27}$$

where

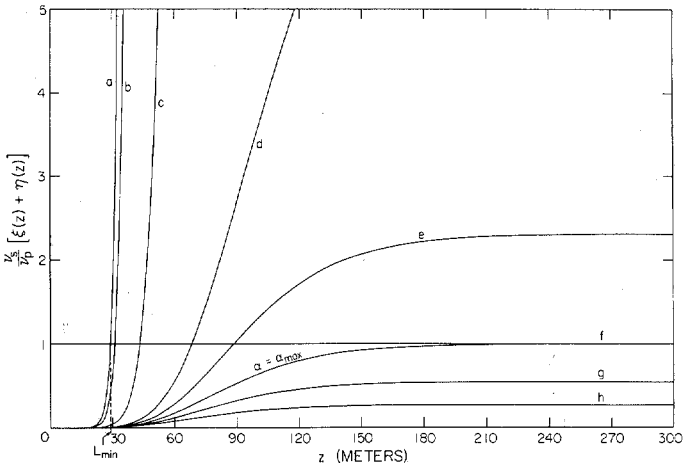


Fig. 1. $(\nu_s/\nu_p)[\xi(z) + \eta(z)]$ for curve $a$ $\alpha = 5 \times 10^{-6}$ cm$^{-1}$, for curve $b$ $\alpha = 5 \times 10^{-5}$ cm$^{-1}$, curve $c$ $\alpha = 2 \times 10^{-4}$ cm$^{-1}$, for curve $d$ $\alpha = 3 \times 10^{-4}$ cm$^{-1}$, for curve $e$ $\alpha = 3.25 \times 10^{-4}$ cm$^{-1}$, for curve $f$ $\alpha = \alpha_{max} = 3.445 \times 10^{-4}$ cm$^{-1}$, for curve $g$ $\alpha = 3.6 \times 10^{-4}$ cm$^{-1}$, for curve $h$ $\alpha = 3.8 \times 10^{-4}$ cm$^{-1}$.

$$p' = h\nu_s \frac{\Delta\nu_R}{2} \left( \frac{\pi A}{\gamma_0 P_0} \right)^{1/2},$$

and is independent of $z$. If it is smaller than 1, then as shown in Fig. 3, no significant stimulated conversion from pump to Stokes photons will take place. The expression in (27) equals 1 when $\alpha = \alpha_{max}$, which is defined as

$$\alpha_{max} = \frac{g_s P_0}{A \left[ \ln\left( \frac{P_0}{p'} \right) - \frac{1}{2} \ln(\alpha_{max}) \right]}. \tag{28}$$

$\alpha_{max}$ is therefore the upper limit of fiber loss for efficient photon conversion. Curve $f$ in Fig. 1 shows $(\nu_s/\nu_p)(\xi + \eta)$ at $\alpha_{max}$. For those given input and fiber parameters, $\alpha_{max}$ is 150 dB/km. In the limit $\alpha z \ll 1$.

$$\frac{\nu_s}{\nu_p}(\xi + \eta) = \frac{P'}{P_0} z^{-1/2} \exp\left( \frac{g_s P_0 z}{A} \right) \tag{29}$$

and is independent of $\alpha$. If it is smaller than 1, no significant stimulated conversion will take place, no matter how small $\alpha$ is. The expression in (29) equals 1, i.e., threshold obtains at a fiber length $z = L_{min}$, given by

$$L_{min} = \frac{A}{g_s P_0} \left[ \ln\left( \frac{P_0}{p'} \right) + \frac{1}{2} \ln(L_{min}) \right]. \tag{30}$$

$L_{min}$ is interpreted as the minimum fiber length required for strong conversion even at zero loss. For the case shown in Fig. 1, $L_{min}$ is 29 m. $\alpha_{max}$ and $L_{min}$ are related by the equation

$$\alpha_{max} L_{min} = 1. \tag{31}$$

Fig. 2 shows $P_p(z)$ and $P_s(z)$ for $\alpha = 5 \times 10^{-5}$ cm$^{-1}$ (~20 dB/km), a high conversion efficiency case. We note the severe pump depletion occurring at $z > 30$ m. Fig. 3 shows $P_p(z)$ and $P_s(z)$ for $\alpha_{max}$. In this small conversion efficiency case, $P_p(z)$ varies roughly as $\exp(-\alpha z)$ throughout the whole fiber. In Figs. 2 and 3, we also plotted $P_0 \exp(-\alpha z)$, which, when compared with $P_p(z)$, indicates the region in which a nonde-

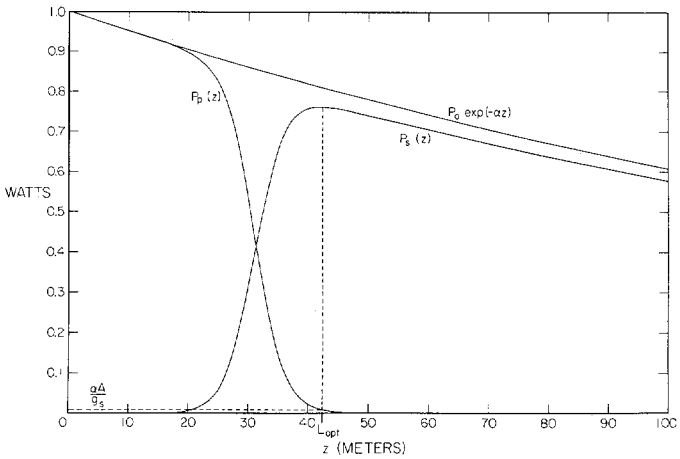


Fig. 2. $P_p(z)$ and $P_s(z)$ for $\alpha = 5 \times 10^{-5}$ cm$^{-1}$.

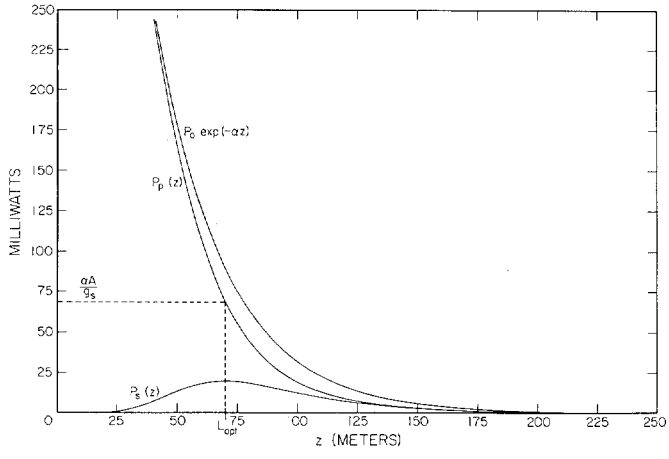


Fig. 3. $P_p(z)$ and $P_s(z)$ for $\alpha = \alpha_{max} = 3.445 \times 10^{-4}$ cm$^{-1}$.

pleted pump approximation is valid. The same input and fiber parameters are used for Figs. 1-3. It is apparent from Figs. 2 and 3 that for a given input pump power, there is an optimal fiber length $L_{opt}$ that results in maximum Stokes power output. Conversely, for a given fiber length $L$, there is an optimal pump power that will give maximum first-order Stokes power output. Maximum Stokes power occurs when $dn_s/dz = 0$. Equation (4) tells us that $n_p \approx \alpha/\gamma_0$ at that point. Thus

$$P_p(L_{opt}) = \frac{\alpha A}{g_s} \tag{32}$$

and from (20)

$$P_s(L_{opt}) = \frac{\nu_s}{\nu_p}\left[P_0 \exp(-\alpha z) - \frac{\alpha A}{g_s}\right]. \tag{33}$$

From these relations, we can readily calculate the optimal pump power or optimal fiber length.

## Comparison with Numerical Solution

To test the validity of our model we solved numerically for $n_p(z)$ and $n_{sj}(z)$ for a particular case assuming a Lorentzian Raman gain profile $\gamma(\nu_j)$ centered on the Stokes frequency $\nu_s$. A Stokes photon input with a Gaussian spectral profile is assumed. It has a bandwidth $\Delta\nu_s$ equal to 800 cm$^{-1}$ centered on $\nu_s$. We divide the frequency space into equal segments 40 cm$^{-1}$ wide. $\gamma$ is then taken to be constant in each segment but different from one segment to another. The behavior of $n_p$ and of the injected Stokes photons is described by the equations

$$\frac{dn_p}{dz} + \alpha_p n_p = -\sum_{j=-10}^{10} \gamma_j (N_{sj} + p) \tag{34}$$

and

$$\frac{dN_{sj}}{dz} + \alpha_s N_{sj} = \gamma_j n_p (N_{sj} + p), \tag{35}$$

where $\gamma_j = \gamma(\nu_j)$.

It is assumed that the input pump photon number is $n_p(z = 0) = 10^{14}$. $N_{sj}$ is the number of Stokes photons in the $j$th frequency segment which is $40j$ cm$^{-1}$ away from $\nu_s$. The initial excitation of the Stokes modes is taken as

$$N_{sj}(z = 0) = 10^{10} \exp\left[-\left(\frac{40j}{\frac{\Delta\nu_s}{2}}\right)^2\right]. \tag{36}$$

The number of Stokes modes in one 40 cm$^{-1}$ segment is $6 \times 10^6$ for a 1 km long fiber. The Raman gain constant of the $j$th segment is

$$\gamma_j = \frac{\gamma_0 \left(\frac{\Delta\nu_R}{2}\right)^2}{(40j)^2 + \left(\frac{\Delta\nu_R}{2}\right)^2} \tag{37}$$

where $\gamma_0$ is $10^{-17}$ cm$^{-1}$ and the Raman linewidth $\Delta\nu_R$ is 400 cm$^{-1}$. The absorption constant of the fiber is assumed to be $\alpha_p = \alpha_s = 10^{-5}$ cm$^{-1}$. Fig. 4 shows the numerical solutions of $N_{sj}(z)$ for $j$ from 0 to 10. The plot for $j = -10$ to 0 is a mirror image and is omitted. In the figure, $10^{-10}\, N_{sj}(z)$ is shown in steps of 5 m from $z = 0$ to $z = 150$ m. At $z = 150$ m, $N_{s0}$ is $2.5 \times 10^{13}$ and it drops, 80 cm$^{-1}$ away, to $N_{s2}$, equal to $8 \times 10^{12}$, indicating a full spectral width at half maximum at $z = 150$ m smaller than 160 cm$^{-1}$. The numerical solution shows that the Stokes wave bandwidth is a function of distance, decreasing with $z$ until maximum conversion is reached. At this point the linear absorption begins to dominate and the bandwidth stays constant for the remainder of the fiber lengths. Fig. 5 shows $n_p(z)$ and $n_s(z)$ obtained both numerically and analytically. The close agreement, especially for large $z$, between the two results is apparent. This justifies the use of the effective bandwidth (6). However, the analytical solution does not yield detailed information about the spectral evolution of the Stokes radiation.

## Comparison with Experiments

As a further test of the validity of the model, our solutions are compared with published experimental results. At small Stokes power, $P_s(L)$ is proportional to $\exp\{(g_s P_0/\alpha A)[1 - \exp(-\alpha L)]\}$. The rapid nonlinear rise in $P_s$ as $P_0$ is increased was indeed observed and reported [3]. Another test is the prediction of threshold pumping power of the single-pass superradiant emission. Threshold occurs when $(\nu_s/\nu_p)\eta = 1$ or

$$\frac{q h \nu_s v_g}{P_{threshold} L} \exp\left\{\frac{g_s P_{threshold}}{\alpha A}[1 - \exp(-\alpha L)]\right\} = 1. \tag{38}$$

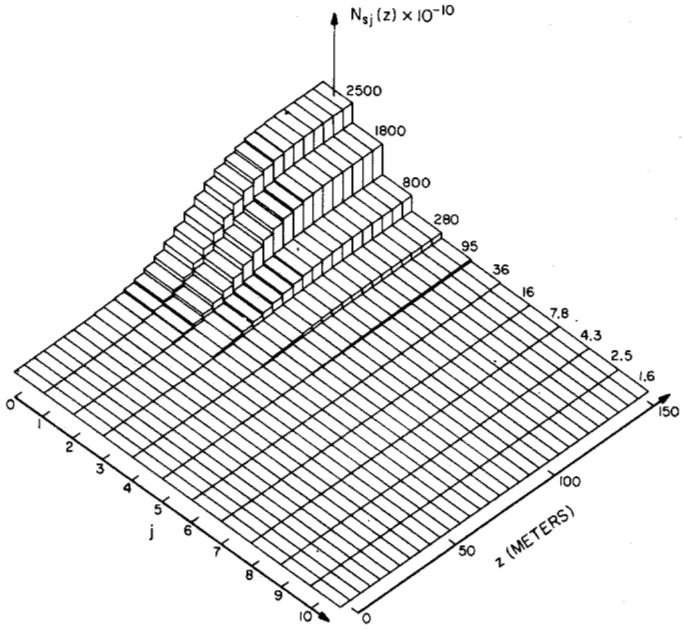


Fig. 4. $N_{sj}(z) \times 10^{-10}$ for $j$ from 0 to 10 and for $z$ from 0 to 150 m.

$q(h\nu_s v_g/L)$ is the power of the fictitious input of 1 photon per mode for the superradiant emission. $q$ is $(n_{\text{eff}}L/c)B_{\text{eff}}$ and $B_{\text{eff}}$ is given by (7). Thus threshold occurs when

$$\frac{h\nu_s \Delta\nu_R}{2P_{\text{threshold}}}\left[\frac{\pi\alpha A}{g_s P_{\text{threshold}}[1-\exp(-\alpha L)]}\right]^{1/2} \cdot \exp\left\{\frac{g_s P_{\text{threshold}}}{\alpha A}[1-\exp(-\alpha L)]\right\} = 1. \tag{39}$$

Consider the case of a recent experiment [14]. A silica fiber, 175 m long with an effective core area of $4.58 \times 10^{-7}$ cm$^2$ was pumped at 1.06 $\mu$m. Stokes wave output was observed at 1.12 $\mu$m. The loss coefficient of the fiber was 4 dB/km ($\alpha = 0.92 \times 10^{-5}$ cm$^{-1}$). $g_s$ was $0.92 \times 10^{-11}$ cm/W and the Raman linewidth $\Delta\nu_R$ was taken to be 400 cm$^{-1}$. Threshold was reported to occur at $P_0 = 70$ W. Our calculation, using (39) and the above data, gives $P_{\text{threshold}} = 58$ W. A similar experiment was performed using a pure-germania ($GeO_2$) core fiber of length 1.5 m and area $7 \times 10^{-8}$ cm$^2$. Stokes output was observed at 1.116 $\mu$m when, again, pumped at 1.06 $\mu$m. The exact value of $g_s$ is not available. It is however known to be ~10 times that of silica [15]. $\Delta\nu_R$ is roughly 100 cm$^{-1}$. The fiber is lossy (300 dB/km) with $\alpha = 6.9 \times 10^{-4}$ cm$^{-1}$. The measured $P_{\text{threshold}}$ was 135 W and our calculation gives 112 W. The agreement with the theory is reasonable. The 20 percent discrepancy may be due to possible polarization scrambling in the fiber or to the presence of backward scattering.

## Conclusion

We have presented a model for describing the forward Raman scattering in single mode fibers. We accounted for pump wave depletion and spontaneous scattering in the model. Analytic solutions of the governing differential equations were obtained. In the limit of negligible pump depletion, our results reduce to those of Smith [11]. The dependence of the pump and Stokes waves' evolution on the fiber losses ($\alpha$) was examined. We showed that a nondepleted pump approximation is valid when

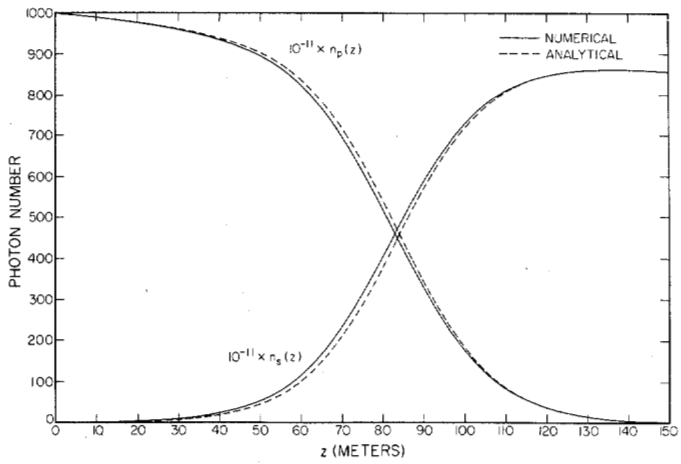


Fig. 5. Numerical and analytical solutions of $10^{-11} \times n_p(z)$ and $10^{-11} \times n_s(z)$.

$\xi + \eta \ll 1$, which is true for large $\alpha$ or short fiber length. In particular, if $\alpha > \alpha_{\max}$, pump power does vary as $\exp(-\alpha z)$ throughout the whole length of even a very long fiber. This may required $\alpha$ to exceed 100 dB/km in some cases and this attenuation factor is larger than that of today's low loss fibers. However, if $L < L_{\min}$, the nondepleted pump approximation is valid even for very low loss fibers. We calculated the optimal pumping power or the optimal fiber length resulting in a maximum first-order Stokes power output. Finally, the theory was compared with experimental results.

## Appendix

To solve (11)

$$\frac{dn_p}{dz} + n_p[\alpha + q\gamma_0 + \gamma_0 n_0 \exp(-\alpha z)] = \gamma_0 n_p^2, \tag{A1}$$

we change variable

$$n_p = \frac{1}{x} \tag{A2}$$

and obtain

$$\frac{dx}{dz} - x[\alpha + q\gamma_0 + \gamma_0 n_0 \exp(-\alpha z)] = -\gamma_0. \tag{A3}$$

Introducing an integrating factor $\exp[-(\alpha + q\gamma_0)z + (\gamma_0 n_0/\alpha)\exp(-\alpha z)]$, we get

$$x = \exp\left[(\alpha + q\gamma_0)z - \frac{\gamma_0 n_0}{\alpha}\exp(-\alpha z)\right]\left\{\int^z -\gamma_0 \cdot \exp\left[-(\alpha + q\gamma_0)z' + \frac{\gamma_0 n_0}{\alpha}\exp(-\alpha z')\right]dz' + C\right\}, \tag{A4}$$

with $C$ as the integration constant to be determined. Using integration by parts,

$$x = \frac{1}{n_0}\exp(\alpha z) + \exp\left[(\alpha + q\gamma_0)z - \frac{\gamma_0 n_0}{\alpha}\exp(-\alpha z)\right]\left\{\int^z \frac{q\gamma_0}{n_0}\exp\left[-q\gamma_0 z' + \frac{\gamma_0 n_0}{\alpha} \cdot \exp(-\alpha z')\right]dz' + C\right\}. \tag{A5}$$

Letting

$$u = \frac{\gamma_0 n_0}{\alpha} \exp(-\alpha z), \tag{A6}$$

the integral in (A5) becomes

$$\frac{-q\gamma_0}{\alpha n_0}\left(\frac{\alpha}{\gamma_0 n_0}\right)^{q\gamma_0/\alpha}\int u^{(q\gamma_0/\alpha)-1}\exp(u)du.$$

This can be integrated easily when the integrand is rewritten in terms of a series. After substituting back (A6), we obtain

$$x = \frac{1}{n_0}\exp(\alpha z)\left\{1 - q\gamma_0 \exp\left[q\gamma_0 z - \frac{\gamma_0 n_0}{\alpha}\exp(-\alpha z)\right] \cdot \sum_{l=0}^{\infty}\frac{\left(\frac{\gamma_0 n_0}{\alpha}\right)^l \exp\left[-(l\alpha + q\gamma_0)z\right]}{(l\alpha + q\gamma_0)l!}\right\}$$
$$+ C\exp\left[(\alpha + q\gamma_0)z - \frac{\gamma_0 n_0}{\alpha}\exp(-\alpha z)\right]. \tag{A7}$$

$C$ is now determined by the initial condition

$$x(z=0) = \frac{1}{n_{p0}}. \tag{A8}$$

Finally, we have

$$n_p = \frac{n_0 \exp(-\alpha z)}{1 + \xi + \eta}, \tag{A9}$$

where

$$\xi = \frac{n_{s0}}{n_{p0}}\exp\left\{q\gamma_0 z + \frac{\gamma_0 n_0}{\alpha}\left[1 - \exp(-\alpha z)\right]\right\}. \tag{A10}$$

and

$$\eta = q\gamma_0 \exp\left[q\gamma_0 z - \frac{\gamma_0 n_0}{\alpha}\exp(-\alpha z)\right] \cdot \sum_{l=0}^{\infty}\frac{\left(\frac{\gamma_0 n_0}{\alpha}\right)^l \left\{1 - \exp\left[-(l\alpha + q\gamma_0)z\right]\right\}}{(l\alpha + q\gamma_0)l!}. \tag{A11}$$

Now

$$n_s = n_0 \exp(-\alpha z) - n_p \tag{A12}$$

from (10). Therefore

$$n_s = n_0 \exp(-\alpha z)\frac{\xi + \eta}{1 + \xi + \eta}. \tag{A13}$$

$n_{sj}$ can now be written down by inspection. It is verified that

$$n_{sj} = \frac{n_0 \exp(-\alpha z)}{1 + \xi + \eta}\left(\frac{n_{sj0}}{n_{s0}}\xi + \frac{1}{q}\eta\right). \tag{A14}$$

## Acknowledgment

We thank D. Shenton for his assistance in computer programming.

## References

[1] E. P. Ippen, "Low-power quasi-cw Raman oscillator," *Appl. Phys. Lett.*, vol. 16, p. 303, 1970.
[2] E. P. Ippen and R. H. Stolen, "Simulated Brillouin scattering in optical fibers," *Appl. Phys. Lett.*, vol. 21, p. 539, 1972.
[3] J. Stone, "CW Raman fiber amplifier," *Appl. Phys. Lett.*, vol. 26, p. 163, 1975.
[4] K. O, Hill, B. S. Kawasaki, and D. C. Johnson, "Low-threshold cw Raman laser," *Appl. Phys. Lett.*, vol. 29, p. 181, 1976.
[5] D. C. Johnson, K. O. Hill, B. S. Kawasaki, and D. Kato, "Tunable Raman fiber-optic laser," *Electron. Lett.*, vol. 13, p. 53, 1977.
[6] R. K. Jain, C. Lin, R. H. Stolen, W. Pleibel, and P. Kaiser, "A high-efficiency tunable cw Raman oscillator," *Appl. Phys. Lett.*, vol. 30, p. 162, 1977.
[7] R. K. Jain, C. Lin, R. H. Stolen, and A. Ashkin, "A tunable multiple Stokes cw fiber Raman oscillator," *Appl. Phys. Lett.*, vol. 31, p. 89, 1977.
[8] C. Lin, R. H. Stolen, W. G. French, and T. G. Malone, "A cw tunable near-infrared (1.085 – 1.175 μm) Raman oscillator," *Opt. Lett.*, vol. 1, p. 96, 1977.
[9] R. H. Stolen, C. Lin, and R. K. Jain, "A time-dispersion-tuned fiber Raman oscillator," *Appl. Phys. Lett.*, vol. 30, p. 340, 1977.
[10] C. Lin, R. H. Stolen, and L. G. Cohen, "A tunable 1.1 μm fiber Raman oscillator," *Appl. Phys. Lett.*, vol. 31, p. 97, 1977.
[11] R. G. Smith, "Optical power handling capacity of low loss optical fibers as determined by stimulated Raman and Brillouin scattering," *Appl. Opt.*, vol. 11, p. 2489, 1972.
[12] A. Yariv, *Quantum Electronics*, 2nd ed. New York: Wiley, 1975.
[13] R. H. Stolen and E. P. Ippen, "Raman gain in glass optical waveguides," *Appl. Phys. Lett.*, vol. 22, p. 276, 1973.
[14] C. Lin, L. G. Cohen, R. H. Stolen, G. W. Tasker, and W. G. French, "Near-infrared sources in the 1 – 1.3 μm region by efficient stimulated Raman emission in glass fibers," *Opt. Commun.*, vol. 20, p. 426, 1977.
[15] M. Hass, "Raman spectra of vitreous silica, germania and sodium silicate glasses," *J. Phys. Chem. Solids*, vol. 31, p. 415, 1970.